Angular-dependent vortex pinning mechanism in $YBa_2Cu_3O_{7-\delta}$ / YSZ quasi-multilayer

Lin Peng, Chuanbing Cai, Changzhao Chen, Zhiyong Liu, Ruben Hühne, and Bernhard Holzapfel

Citation: Journal of Applied Physics **104**, 033920 (2008); doi: 10.1063/1.2968235
View online: http://dx.doi.org/10.1063/1.2968235
View Table of Contents: http://scitation.aip.org/content/aip/journal/jap/104/3?ver=pdfcov
Published by the AIP Publishing

Angular-dependent vortex pinning mechanism in $YBa_2Cu_3O_{7-\delta}$/YSZ quasi-multilayer

Lin Peng,[1,a)] Chuanbing Cai,[1] Changzhao Chen,[1] Zhiyong Liu,[1] Ruben Hühne,[2] and Bernhard Holzapfel[2]
[1]*Physics Department, Shanghai University, Shanghai 200444, People's Republic of China*
[2]*Leibniz Institute for Solid State and Materials Research, Helmholtzstrasse 20, 01069 Dresden, Germany*

(Received 26 March 2008; accepted 12 June 2008; published online 13 August 2008)

The temperature and magnetic field dependences of anisotropic pinning contributions of $YBa_2Cu_3O_{7-\delta}$/YSZ quasi-multilayer have been investigated by the measurement of angular-dependent critical current density (J_c). With the isotropic and anisotropic pinning contributions in a wide range of temperature, we identify the possible sources of the pinning centers and classify them into the weak and the strong flux pinning model. Angular-dependent $J_c(H,T)$ measurements have demonstrated that the growth control strategy is very effective in preventing the vortex motion at high fields and high temperatures. It is suggested that at high applied fields, such as 7 T, the pinning contribution of the nanostructured quasi-multilayers is dominated by the anisotropic disorders, while at intermediate-low fields (such as 1 T) the pinning contribution is determined by both isotropic and anisotropic disorders, suggesting the coexistence of isotropic and anisotropic pinning. © *2008 American Institute of Physics*. [DOI: 10.1063/1.2968235]

I. INTRODUCTION

It is well known that due to the elimination of weak links and the emergence of as-grown flux pinning centers such as dislocations, the epitaxial $YBa_2Cu_3O_{7-\delta}$(YBCO) thin films may show a very high superconducting critical current density (J_c) and a high irreversibility field (H_{irr}) at the temperature of liquid nitrogen.[1,2] Coated conductors based on YBCO epitaxial films now appear very promising for power applications because of the tremendous advances in understanding of both physics and materials science.[3] However, the highest critical current densities observed so far in YBCO films and related coated conductors are still much below the maximum theoretical limit (that is, $\sim 1\%-10\%$ of the depairing current J_0).[4] To explore the possibility of improvement in J_c and in-field behavior, great efforts have been made to add the artificial flux pinning centers in the YBCO thin films, which normally enhance an effective immobilization of vortices in a dense structure of defects with nanometer dimensions.

Recently, several strategies for the preparation of nanostructured YBCO films have been proposed to increase flux pinning, including chemical doping (e.g., to change the initial compositions of physical vapor deposition targets),[5,6] growth control (e.g., to build up multilayers or incomplete multilayers),[7,8] and substrate modulation (e.g., to introduce nanoscale islands of a second phase onto the substrate).[9,10] Among them, growth controlling is very attractive as it can provide a high density of second-phase defects of up to 10^{11} cm^{-2}.[11] However, it is commonly observed that there are competitive contributions between zero-field J_c and in-field J_c coming from chemical doping or secondary phase additions. This, together with anisotropic microstructures, implies that the flux pinning mechanism in such nanostructured YBCO thin films, may be complex, far away from a complete understanding. Thus the anisotropic flux pinning contribution shows the ongoing interests and importance for the zero-field and in-field J_c behavior of RE123 thin films as well as coated conductors.

In the present work, a kind of growth-controlled quasi-multilayer consisting of YBCO and yttria-stabilized zirconia (YSZ) is prepared with a given ratio of the two compounds. Electrotransport measurements are made at different temperatures, magnetic fields (H), as well as angle (Θ) between the c-axis orientation and magnetic field direction. A methodology based on angular-dependent J_c measurement is proposed,[12] enabling us to identify and quantify the dominant pinning contributions depending on the dimensionality of the defects.

II. EXPERIMENTAL DETAILS

Quasi-multilayers in the name of $p(m\mathrm{YBCO}/n\mathrm{YSZ})$ are prepared by means of pulsed-laser deposition (PLD) using commercial stoichiometric targets and single crystal substrates of (001) $SrTiO_3$, where m and n denote the number of laser pulses on YBCO and YSZ, respectively, and p is the repetition number of YBCO/YSZ bilayers, i.e., periodic number for each consequential layer. A Lambda Physik KrF excimer laser ($\lambda = 248$ nm) runs at a repetition rate of 5 Hz with an energy density of 2.4–3.0 J/cm^2 alternatively on the two targets. The standard deposition parameters for YBCO are applied, with a heater temperature of 820 °C, a background pressure of 0.3 mbar O_2, and oxygen loading of 400 mbar. These conditions result in an YBCO growth rate of about 1 Å/pulse. Thus, 40 pulses of YBCO give roughly 3.5 unit cell thickness. During the laser deposition, several pulses on the YSZ target give no rise to a complete layer of heterogeneous phases. This results in a so-called quasi-multilayer consisting of YBCO film matrix and islandlike

a)Electronic mail: plpeng@shu.edu.cn.

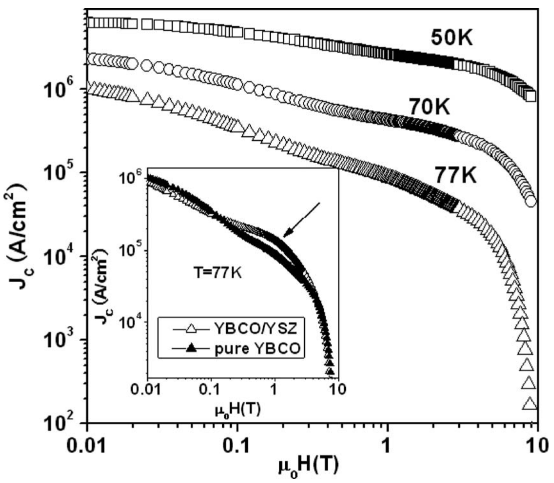

FIG. 1. Magnetic-field dependence of J_c at three given temperatures (50, 70, and 77 K) for the YBCO/YSZ quasi-multilayer. The inset shows a comparison between a pure Y123 film and a quasi-multilayer at 77 K. The arrow indicates the extra bump around 1 T for the quasi-multilayer.

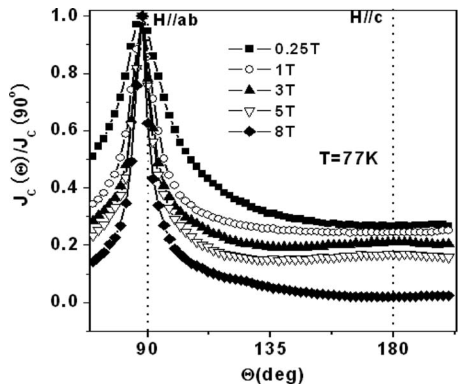

FIG. 2. Angular dependence of $J_c(\Theta)/J_c(90°)$ for the YBCO/YSZ quasi-multilayer sample at 77 K and in several magnetic fields.

$BaZrO_3$ nanoparticles. More details for sample preparation and structural features can be found in our previous publications.[13]

Critical current density J_c was measured in various magnetic fields (Quantum Design PPMS) by the standard four-probe method on a bridge of 0.8 mm length and 50 μm width, patterned by photolithography. The angular dependence of J_c was measured in a maximum force configuration, i.e., the sample was rotated around the current axis to achieve various angles Θ between the c-axis orientation and the magnetic field direction. The electric field criterion of $E_c = 10^{-6}$ V/cm was used for all J_c determinations.

III. RESULTS AND DISCUSSION

According to the previous x-ray diffraction and atomic force microscopy measurements,[13] the YBCO/YSZ quasi-multilayers prepared by PLD show good c-axis orientations and nanosized heterogeneous perovskite phase of $BaZrO_3$. Figure 1 shows the magnetic-field dependence of $J_c(H \| c)$ at three typical temperatures of 50, 70, and 77 K for the quasi-multilayer with $m=40$, $n=2$, and $p=70$. As seen in the inset of Fig. 1, the sample has a higher value of J_c at intermediate-high fields, showing a characteristic bump at intermediate magnetic fields, in contrast to the pure YBCO films. This implies that the increased flux pinning occurs as a result of YSZ doping.

In order to give insight into the flux pinning mechanism of such a quasi-multilayer, we study the angular dependence of J_c. As shown in Fig. 2, a strong main peak is present at $H \| (a,b)$, whereas a smoother and weaker second peak is observed as well at $H \| c$. Generally the (a,b) plane peak is attributed to intrinsic pinning, mainly resulting from the CuO_x planes and the others such as extrinsic linear or planar defects parallel to (a,b) planes.[14,15] In contrast, the second peak at $H \| c$ is probably due to the correlated defects parallel to the c-axis, such as twin planes, and edge and screw dislocations.[16,17] So far, the defects mentioned above may be sorted as anisotropic in the sense that their contribution to J_c depends on the direction of the applied magnetic field. Note that the two types of anisotropic defects, aligned with (a,b) planes and c axis, are both low dimensional, hence, being effective for flux pinning.[12]

It is possible to identify the contributions from either the anisotropic defects or isotropic defects through the analysis on the angular dependence of $J_c(H,T)$. The anisotropic defects may modify the anisotropy factor of the electronic mass and then the J_c, depending on the angle between the directions of applied field and transport current.[18,19] On the contrary, the contribution of the isotropic defects to the critical current density is independent of the direction of the applied magnetic field as the isotropic defects hardly modify the anisotropy factor of the electronic mass of YBCO.

The isotropic and anisotropic behaviors of the nanocomposite films may be characterized based on the scaling behavior of $J_c(H,\Theta)$ at fixed temperatures. As proposed by Blatter *et al.*,[20] the $J_c(H,\Theta)$ results obtained for isotropic pinning centers may be applicable to describe the anisotropic materials with a simple variable of effective fields ($\tilde{H}_{\mathrm{eff}}$). The scaling approach was initially applied to coated conductors by Kim *et al.*[15] If flux pinning is caused by isotropic defects (uncorrelated pinning), J_c depends on H and Θ only through a single variable and it can be written as follows:[21]

$$J_c^{\mathrm{is}}(H,\Theta) = J_c^{\mathrm{is}}(\tilde{H}_{\mathrm{eff}}), \tag{1}$$

$$\tilde{H}_{\mathrm{eff}} = H\varepsilon(\Theta), \tag{2}$$

$$\varepsilon(\Theta) = (\cos^2\Theta + \gamma^{-2}\sin^2\Theta)^{1/2}. \tag{3}$$

In these equations, $\gamma = (m_c/m_a)^{1/2} \approx 5-7$ is the mass anisotropy, where m_c and m_a are the Ginzburg–Landau effective masses for pair motion along the c direction and the (a,b) plane, respectively.[18] Thus, for those H-Θ regions where only uncorrelated pinning is present, $J_c(H,\Theta)$ curves should collapse onto a single one if it is plotted as a function of $\tilde{H}_{\mathrm{eff}}$. This approach only explains qualitatively whether uncorrelated pining is present in some H-Θ region, but it does not provide the function $J_c^{\mathrm{is}}(\tilde{H}_{\mathrm{eff}})$.[16]

To test the validity of the scaling for some H-Θ regions, we mapped the J_c curves for each $\tilde{H}_{\mathrm{eff}}$. It is concluded that the scaling can be achieved with $\gamma \sim 7$ for the present nano-

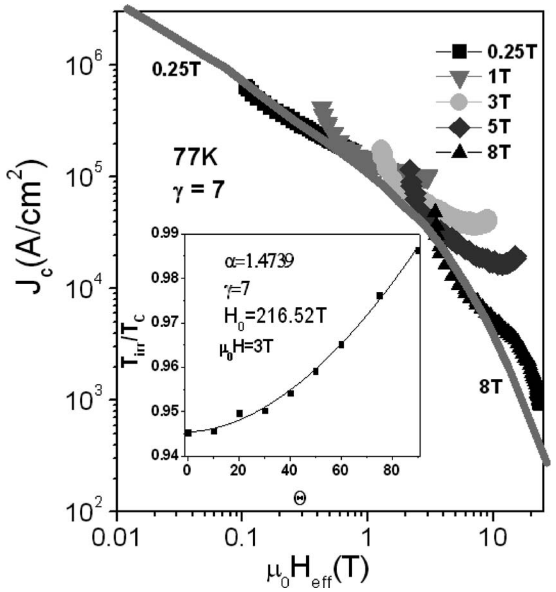

FIG. 3. Scaling behavior of $J_c(\Theta)$ as a function of $H_{\rm eff}$ at 77 K. The solid line is a fit based on the scaling theory for different magnetic fields. The inset shows the anisotropy of the irreversibility line in the magnetic field of 3 T. The solid line represents the fitting to $\varepsilon(\Theta)H_{\rm irr}(\Theta,T_{\rm irr})=H_0[1-(T_{\rm irr}/T_c)]^{\alpha}$ with $\gamma=7$.

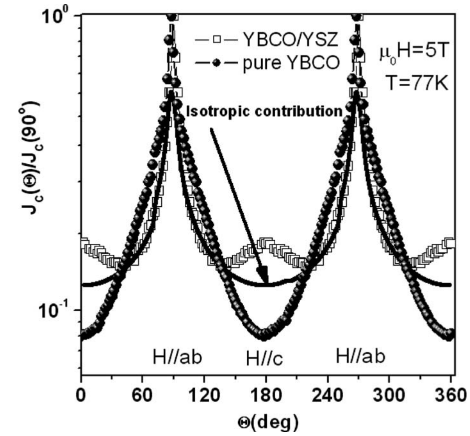

FIG. 4. $J_c(\Theta)/J_c(90°)$ for the YBCO/YSZ quasi-multilayer sample at 77 K and 5 T. The solid line is a fit according to the original Tachiki–Takahashi model (Ref. 21), i.e., $J_c(\Theta)=J_c(0)|\cos\Theta|^{-0.5}$. Aside from the main peak at $H\|(a,b)$, the second peak appears at $H\|c$.

composite films. We use $\gamma\sim 7$ as the only adjustable parameter and then find that all the curves of J_c-T in various magnetic fields collapse into a single one if they are plotted (see the Fig. 3), except those regions with the angles close to $H\|(a,b)$ or $H\|c$. The part of the cure which contains the collapsed data shows the isotropic defect contribution $J_c^{\rm is}(\tilde{H}_{\rm eff})$. According to the scaling approach above, the anisotropic irreversibility line (IL) of $H_{\rm irr}(\Theta,T_{\rm irr})$ may be described by the expression as follows:[12]

$$\varepsilon(\Theta)H_{\rm irr}(\Theta,T_{\rm irr}) = H_0\left(1-\frac{T_{\rm irr}}{T_c}\right)^{\alpha}. \quad (4)$$

The inset of Fig. 3 shows an IL, where $\gamma\sim 7$ and $\mu_0H=3$ T. Notice that at the IL, the angular dependence of irreversibility field indicates the increased anisotropy.

On the other hand, one may estimate the intrinsic flux pinning contribution to $J_c(\Theta)$ according to the model of Tachiki and Takahashi,[22] giving $J_c(\Theta)=J_c(0)|\cos\Theta|^{-0.5}$. The model is well suited for higher electronic anisotropies. It can be used for YBCO, as shown already by Tachiki and Takahashi,[22] however, at very low temperatures, where the coherence length is short and the superconducting layers are well separated. An example for $\mu_0H=5$ T and $T=77$ K is shown in Fig. 4. The model shows a good fit for the angles around 90° or 270°, i.e., the region of $H\|(a,b)$ plane. In view of isotropic defects and mass anisotropy, however, it seems hard to understand that the second peak emerged at the region of $H\|c$. The fitting discrepancy at this angle regions suggests that there may exist correlated defects along the c-axis. They may act as correlated pinning centers, giving rise to the second set of peaks. This may be also the reason for the bump in J_c-H curves plotted in a log-log scale (see the inset of Fig. 1).

To further understand the flux pinning mechanisms of the present quasi-multilayer, we evaluate the isotropic and anisotropic contributions to J_c in a wide range of magnetic fields and temperatures. According to the Blatter model,[21] the temperature dependence of the critical current density for weak isotropic flux pinning centers usually exhibit an exponential decrease with temperature. This may be described by[21]

$$J_c^{\rm WP}(T) = J_c^{\rm WP}(0)e^{-T/T_0}. \quad (5)$$

In contrast, the strong anisotropic flux pinning mechanism is developed to analyze the flux pinning related to correlated disorders. The J_c-T behavior with respect to anisotropic flux pinning centers may be well described as follows:[23]

$$J_c^{\rm SP}(T) = J_c^{\rm SP}(0)e^{-3(T/T^*)^2}. \quad (6)$$

This normally gives rise to a smoother temperature dependence.[21,24] In low magnetic fields, a mixed behavior can be explained by using the sum of two contributions, i.e.,

$$J_c^{\rm MP}(T) = J_c^{\rm WP}(0)e^{-T/T_0} + J_c^{\rm SP}(0)e^{-3(T/T^*)^2}, \quad (7)$$

where $J_c^{\rm WP}(0)$ and $J_c^{\rm SP}(0)$ are the critical current densities at 0 K for weak and strong pinning, respectively, and T_0 and T^* are characteristic temperatures which fix the energy scale of the pinning centers for each contribution. Figure 5 shows the temperature dependence of $J_c(T)$ in two given magnetic fields ($H\|c$). The solid line is the fit based on the mixed flux pinning mechanism in the magnetic field of 1 T. The dash line is the fit based on the strong anisotropic flux pinning mechanism in the high field of 7 T. It is found that the J_c-T relationship at 7 T can be very well described by Eq. (6), where $J_c^{\rm SP}(0)$ and T^* are 5.787 MA/cm^2 and 65.06 K, respectively. This implies that strong-anisotropic flux pinning may dominate the overall $J_c(H)$ in high applied fields such as 7 T. Thus, in high magnetic fields, the dominant contribution is determined by the anisotropic disorders. Meanwhile, a mixed behavior at 1 T is observed and the J_c data can also be well described by Eq. (7), where $J_c^{\rm WP}(0)$, $J_c^{\rm SP}(0)$, T_0, and T^* are 20.0 MA/cm^2, 10.5 MA/cm^2, 4.16 K, and 70.40 K, respectively. Therefore, it seems reasonable to identify the

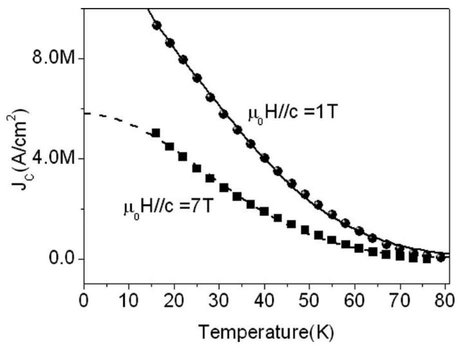

FIG. 5. Temperature dependence of $J_c(T)$ in two different magnetic fields ($H \| c$). The solid line is the fit based on the mixed flux pinning mechanism in the magnetic field of 1 T. The dash line is the fit based on the strong anisotropic flux pinning mechanism in the high field of 7 T.

weak flux pinning contribution as well as the strong flux pinning contribution based on the measured temperature dependence of critical current density. Figure 6 shows the two separated contributions for the studied quasi-multilayer at 1 T, and the inset of Fig. 6 gives the fitting results based on the Eq. (7) at 1 T. A sharp drop occurs due to the proximity of the irreversibility line at the region close to 80 K (see the inset of Fig. 6). Notice that weak isotropic pinning contribution appears dominant at very low temperatures, while with increasing temperature there is an inversion of the weights from the weak isotropic pinning contributions to the strong anisotropic pinning contributions. Thus, above ~10 K the dominant contribution comes from the correlated disorder generating the characteristic bump in the temperature dependence of the critical current density. On the other hand, the existing bump at high temperatures in the semilogarithmic plots (see the inset of Fig. 6) clearly shows that J_c^{WP} gets vanishingly small and J_c^{SP} completely controls the behavior of J_c at the region close to the IL.[12,25]

IV. CONCLUSIONS

Magnetotransport measurements of J_c have demonstrated that the growth control strategy is very effective in

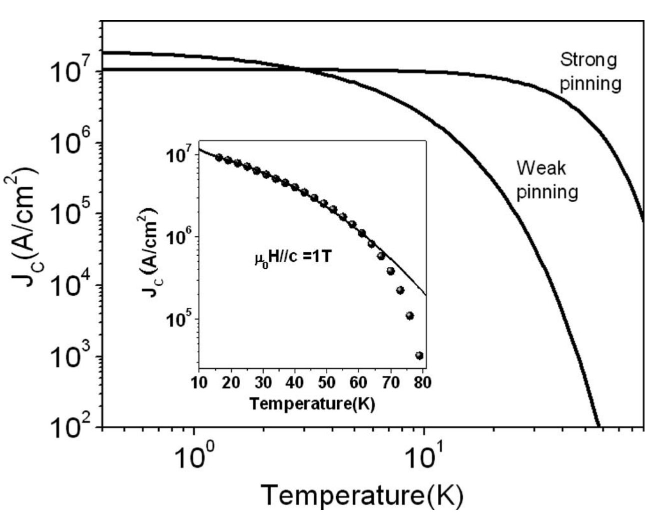

FIG. 6. Separation of weak and strong flux pinning contributions for the YBCO/YSZ quasi-multilayer in the field of 1 T. The inset shows the J_c data and the fit according to Eq. (7).

preventing the vortex motion at high fields and high temperatures. Angle-dependent $J_c(H,T)$ reveals that the presence of a second J_c peak at $H \| c$ is caused by c-axis correlated defects. Based on the existing anisotropic flux theory, we have identified the isotropic and the anisotropic defects and evaluated their contributions to the critical current densities subject to applied magnetic fields and temperature. It is evident that the studied quasi-multilayers give rise to anisotropic structural disorders, leading to enhanced critical current density at high fields, which is essential for power application of coated conductors.

ACKNOWLEDGMENTS

This work was partly sponsored by the National Natural Science Foundation of China (Grant Nos. 5062057 and 10774098), the National Science Foundation of China, the Ministry of Science and Technology of China (973 Projects) (Grant No. 2006CB601005), the Science and Technology Commission of Shanghai Municipality (Grant No. 0752nm017), Shanghai Leading Academic Discipline Project (Project No. T0104), and the Project Based Personnel Exchange Programme with China and Germany (PPP) (Project No. [2006] 3139).

[1]Ch. Jooss, R. Warthmann, and H. Kronmüller, Phys. Rev. B **61**, 12433 (2000).
[2]M. Parans Paranthaman and T. Izumi, MRS Bull. **29**, 533 (2004).
[3]B. Dam, J. M. Huijbregtse, F. C. Klaassen, R. C. F. van der Geest, G. Doornbos, J. H. Rector, A. M. Testa, S. Freisem, J. C. Martinez, B. Stäuble-Pümpin, and R. Griessen, Nature (London) **399**, 439 (1999).
[4]J. Gutierrez, A. Llordes, J. Gazquez, M. Gibert, N. Roma, S. Ricart, A. Pomar, F. Sandiumenge, N. Mestres, T. Puig, and X. Obradors, Nat. Mater. **6**, 367 (2007).
[5]J. L. MacManus-Driscoll, S. R. Foltyn, Q. X. Jia, H. Wang, A. Serquis, B. Maiorov, L. Civale, Y. Lin, M. E. Hawley, M. P. Maley, and D. E. Peterson, Appl. Phys. Lett. **84**, 5329 (2004).
[6]J. L. MacManus-Driscoll, S. R. Foltyn, Q. X. Jia, H. Wang, A. Serquis, L. Civale, B. Maiorov, M. E. Hawley, M. P. Maley, and D. E. Peterson, Nat. Mater. **3**, 439 (2004).
[7]C. Cai, B. Holzapfel, J. Hänisch, and L. Schultz, Phys. Rev. B **70**, 212501 (2004).
[8]T. Haugan, P. N. Barnes, R. Wheeler, F. Meisenkothen, and M. Sumption, Nature (London) **430**, 867 (2004).
[9]K. Matsumoto, T. Horide, K. Osamura, M. Mukaida, Y. Yoshida, A. Ichinose, and S. Horii, Physica C **412**, 1267 (2004).
[10]K. Matsumoto, T. Horide, A. Ichinose, S. Horii, Y. Yoshida, and M. Mukaida, Jpn. J. Appl. Phys., Part 2 **44**, L246 (2005).
[11]P. N. Barnes, T. J. Haugan, C. V. Varanasi, and T. A. Campbell, Appl. Phys. Lett. **85**, 4088 (2004).
[12]J. Gutierrez, T. Puig, and X. Obradors, Appl. Phys. Lett. **90**, 162514 (2007).
[13]L. Peng, C. Cai, C. Chen, Z. Liu, J. Liu, B. Gao, and J. Zhang, J. Phys. D **41**, 155403 (2008).
[14]L. Civale, B. Maiorov, J. L. Manus-Driscoll, H. Wang, T. G. Holesinger, S. R. Foltyn, A. Serquis, and R. N. Arendt, IEEE Trans. Appl. Supercond. **15**, 2808 (2005).
[15]S. I. Kim, A. Gurevich, X. Song, X. Li, W. Zhang, T. Kodenkandath, M. Rupich, T. G. Holesinger, and D. Larbalestier, Supercond. Sci. Technol. **19**, 968 (2006).
[16]L. Civale, B. Maiorov, A. Serquis, J. O. Willis, J. Y. Coulter, H. Wang, Q. X. Jia, P. N. Arendt, J. L. Manus-Driscoll, M. P. Maley, and S. R. Foltyn, Appl. Phys. Lett. **84**, 2121 (2004).
[17]A. Palau, J. H. Durrell, J. L. MacManus-Driscoll, S. Harrington, T. Puig, F. Sandiumenge, X. Obradors, and M. G. Blamire, Phys. Rev. Lett. **97**, 257002 (2006).
[18]D. E. Farrell, J. P. Rice, D. M. Ginsberg, and J. Z. Liu, Phys. Rev. Lett. **64**, 1573 (1990).

[19]W. K. Kwok, S. Fleshler, U. Welp, V. M. Vinokur, J. Downey, G. W. Crabtree, and M. M. Miller, Phys. Rev. Lett. **69**, 3370 (1992).
[20]G. Blatter, V. B. Geshkenbein, and A. I. Larkin, Phys. Rev. Lett. **68**, 875 (1992).
[21]G. Blatter, M. V. Feigelman, V. B. Geshkenbein, A. I. Larkin, and V. M. Vinokur, Rev. Mod. Phys. **66**, 1125 (1994).
[22]M. Tachiki and S. Takahashi, Solid State Commun. **72**, 1083 (1989).
[23]B. Martinez, X. Obradors, A. Gou, V. Gomis, S. Pinol, J. Fontcuberta, and H. Van Tol, Phys. Rev. B **53**, 2797 (1996).
[24]D. R. Nelson and V. M. Vinokur, Phys. Rev. B **48**, 13060 (1993).
[25]J. Plain, T. Puig, F. Sandiumenge, X. Obradors, and J. Rabier, Phys. Rev. B **65**, 104526 (2002).